

Article

Electrode Microbial Communities Associated with Electron Donor Source Types in a Bioelectrochemical System Treating Azo-Dye Wastewater

Zechong Guo^{1,2,3}, Lu Zhang¹, Min-Hua Cui^{2,4,*} and Aijie Wang^{2,5,*}

¹ School of Environmental and Chemical Engineering, Jiangsu University of Science and Technology, Zhenjiang 212100, China; guozhong@just.edu.cn (Z.G.); avavip@126.com (L.Z.)

² State Key Laboratory of Urban Water Resource and Environment, Harbin Institute of Technology, Harbin 150090, China

³ Jiangxi Jindalai Environmental Protection Co., Ltd., Nanchang 330100, China

⁴ School of Environmental and Civil Engineering, Jiangnan University, Wuxi 214122, China

⁵ Key Laboratory of Environmental Biotechnology, Research Center for Eco-Environmental Sciences, Chinese Academy of Sciences, Beijing 100085, China

* Correspondence: cuiminhua@jiangnan.edu.cn (M.-H.C.); waj0578@hit.edu.cn (A.W.)

Abstract: Bioelectrochemical systems (BESs) have been acknowledged to be an efficient technology for refractory pollution treatment. An electron donor is as an indispensable element of BES, and domestic wastewater (DW) has been proved as a cost-efficient and accessible alternative option to expensive carbon sources (such as acetate and glucose), yet its effect on microbial community evolution has not been thoroughly revealed. In this study, the electrode microbial communities from BESs treating azo dye wastewater fed by DW (R_{DW}), acetate (R_{Ac}), and glucose (R_{Glu}) were systematically revealed based on 16S rRNA Illumina MiSeq sequencing platform. It was found that there were significant differences between three groups in microbial community structures. *Desulfovibrio*, *Acinetobacter*, and *Klebsiella* were identified as the predominant bacterial genera in R_{DW} , R_{Ac} , and R_{Glu} , respectively. *Methanosaeta*, the most enriched methanogen in all reactors, had a relative lower abundance in R_{DW} . Microbial communities in R_{Ac} and R_{Glu} were sensitive to electrode polarity while R_{DW} was sensitive to electrode position. Compared with pure substrates, DW increased the diversity of microbial community and, thus, may enhance the stability of electrode biofilm. This study provides an insight into the microbial response mechanism to the electron donors and provides engineering implications for the development of BES.

Keywords: bioelectrochemical system (BES); electron donor source; canonical correspondence analysis; microbial community structure



Citation: Guo, Z.; Zhang, L.; Cui, M.-H.; Wang, A. Electrode Microbial Communities Associated with Electron Donor Source Types in a Bioelectrochemical System Treating Azo-Dye Wastewater. *Water* **2022**, *14*, 1505. <https://doi.org/10.3390/w14091505>

Academic Editors: Andrea G. Capodaglio and Goen Ho

Received: 18 March 2022

Accepted: 5 May 2022

Published: 7 May 2022

Publisher's Note: MDPI stays neutral with regard to jurisdictional claims in published maps and institutional affiliations.



Copyright: © 2022 by the authors. Licensee MDPI, Basel, Switzerland. This article is an open access article distributed under the terms and conditions of the Creative Commons Attribution (CC BY) license (<https://creativecommons.org/licenses/by/4.0/>).

1. Introduction

Electrochemical technologies are proved as an efficient method for contamination remediation by electrochemical oxidation and electrochemical reduction processes [1,2]. However, the high cost and extreme operating conditions impede wide applications in the practical scene. Considering the cost-efficient and feasibility of large-scale capability, biological treatment is still the most widely used wastewater treatment technology. However, it was difficult to satisfy the stricter discharging standard due to the low efficiency and complicated manipulation, especially in treating refractory industrial wastewaters, such as azo dye wastewater, chemical wastewater, etc. Introducing electrochemical technology into conventional biological facilities seems to be a potential strategy to deal with wastewater issues [3]. The bioelectrochemical system (BES) is a rapidly developing technology that inherits both the advantages of electrochemical and biological processes. The feasibility and superiority of implementing BES to remediate pollution have been verified in covering azo dyes, nitro compounds and metals reduction, and dehalogenation [4]. Among them, azo

dye decolorization is one of the most successful applications of BES in industrial wastewater treatments. Due to the presence of external circuit, the electron transfer process was obviously enhanced and resulted in fast decolorization compared to traditional anaerobic process. For now, several pioneer works have confirmed the feasibility of the practical application of BES technology [4]. However, more efforts are required to promote the industrialized application of BES, such as evaluating the performance under practical scenario, exploring the mechanism of microbial functional stabilization, reducing the operational cost of BES technology, etc.

In a BES, electrochemical active microorganisms (EAMs) play an important role by involving extracellular electron transfer. Electrons are produced by anode respiration bacteria oxidizing organic matters and transferred to the cathode to drive reduction actions. These EAMs can serve as a biocatalyst to decrease applied voltage and increase reaction efficiency. Thus, to maintain a stable microbial community structure capable of achieving efficient electron transfer, pollutant degradation is crucial to the successful operation of a BES. In addition to some common physical and chemical influencing factors [5–10] in BES, the microbial community structure might also be influenced by some special operation parameters, such as electrode position and polarity [4,11], salinity and COD/N [12], applied voltage [13], organic loading rates, and electron donors. In previous studies, simple and pure carbon sources such as acetate, glucose, and yeast extract are commonly employed to support BES's operation, but they comprise diseconomy and are impracticable to access in the large-scale application scene. To decrease operating costs, various organic wastes/wastewater were proposed to serve as alternative electron donors to drive bioelectrochemical reactions. Among them, domestic wastewater (DW) has been proved to be a cost-effective yet highly efficient electron donor source in a BES treating azo dye wastewater in our previous study [14]; nevertheless, the characteristics of the microbial community structure of electrode biofilm with DW as a carbon source has not been thoroughly revealed. Therefore, this study systematically analyzed the effects of various electron donors (including acetate, glucose, and DW) on microbial community structure by conducting 16S rRNA Illumina Miseq sequencing and evaluated the feasibility and superiority of DW as electron donor at the level of microbial community evolution.

2. Materials and Methods

2.1. Reactor Configuration and Operation

Three identical cylindrical reactors were manufactured with plexiglass [14]. Each one had a working volume of approximately 1.25 L ($ID \times L = 8 \text{ cm} \times 25 \text{ cm}$) (see Figure 1). Two pairs of electrodes were installed into the reactor, from the bottom to the top, which was arranged as down-cathode, down-anode, up-cathode, and up-anode with the distance of 2.5 cm between each electrode. Both anodes and cathodes were constructed by granular graphite (diameter from 3 to 6 mm) with 8 cm in diameter and 4 cm in height, producing the total electrode volume of 200 cm^3 . Before use, granular graphite was washed by soaking in 32% HCl four times to remove foreign materials [15]. The graphite rod ($\Phi = 4 \text{ mm}$) penetrated the electrode zone and worked as an electron collector. A saturated calomel electrode (SCE, +247 mV vs. standard hydrogen electrode) was used as the reference electrode. During all experiments, a voltage of 0.5 V was supplied between the anode and cathode by a DC power supply. A 10Ω resistor was connected in series into the electric circuit. The voltages across this resistor were recorded every 10 min by a data acquisition system (Keithley 2700), which were automatically converted to the current according to Ohm law.

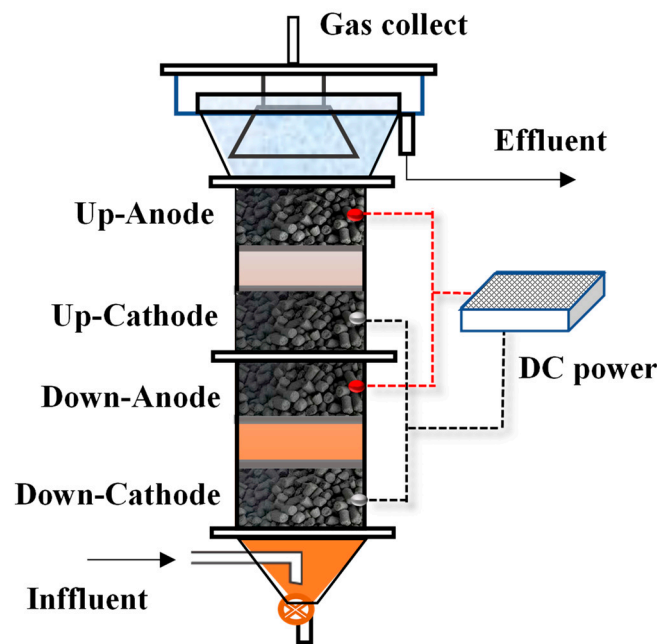


Figure 1. Schematic representation of the reactor [14].

All three reactors were startup in batch mode. Effluent collected from a long-term operated single chamber BES was amended with sodium acetate (NaAc, 1000 mg/L) and acid orange 7 (AO7, 200 mg/L) as the inoculum solution. In the first batch operation cycle, 50 mL anaerobic activated sludge (SS of 35.57 mg/L and VSS of mg/L) was also added into the reactors to strengthen the biomass. After that, the inoculum solution was replaced every two days. When a stable current output was observed, the reactors were considered to be successfully started up. Subsequently, the operation of reactors was changed to continuous flow mode. The hydraulic retention times for all reactors were set at 6 h throughout the experiment. Domestic wastewater (DW) collected from a local sewage well was filtered by a 400-mesh sieve to remove particles that might block the interspace of electrodes. The COD of the filtrated DW was detected as 309 ± 18 mg/L in all experiments, total nitrogen of 59.38 ± 1.54 mg/L, ammonium of 49.68 ± 5.29 mg/L, total phosphorus of 13.14 ± 1.43 mg/L, sulfate of 88.90 ± 11.33 mg/L, chloride of 67.41 ± 18.04 mg/L, alkalinity of 217 ± 75 mg-CaCO₃/L, and pH of 7.39 ± 0.07 . DW was then amended with AO7 (200 mg/L) as the influent of one reactor (R_{DW}). As the controls, the other two reactors were fed with synthetic wastewater with acetate (R_{Ac}) and glucose (R_{Gl}) as the electron donor sources, respectively, which contributed the same COD as that in DW. In addition to the electron donor sources, synthetic wastewater comprised AO7 (200 mg/L) and other minerals, as reported previously [16].

2.2. Chemicals and Analytical Method

The liquid samples were collected every day. AO 7 was used as the model azo dye (purity > 95%, Shanghai Sangon Biotech Co., Ltd., Shanghai, China). Liquid samples taken from reactors were immediately filtered through the 0.45 μm filters (Tianjin Jinteng Experiment Equipment Co., Ltd., Tianjin, China). AO7 concentration was quantified by a UV-Vis spectrophotometer (UV-1800, Shanghai Meipuda instrument Co., Ltd., Shanghai, China) at a wavelength of 484 nm. COD was quantified by the HACH method.

2.3. Biofilm Sampling and High-Throughput 16S rRNA Gene Illumina MiSeq Sequencing

After operating those reactors for more than 200 days, biofilms along with graphite particles were collected from anodes and cathodes, respectively. Graphite particles of each

electrode were sampled from at least 6 positions in different heights and combined for DNA extraction.

Amplicon libraries were constructed by Illumina MiSeq PE 250 using universal primers 515F (5'-GTGCCAGCMGCCGCGGTAA-3') and 806R (5'-GGACTACHVGGGTWTCTAAT-3'). Both forward and reverse primers were added with barcodes. PCR amplification, products purification and quantification, and sequencing were carried out by using the Illumina MiSeq platform in The Beijing Genomics Institute (BGI).

3. Results and Discussion

3.1. Performance of BESs Served with Different Electron Donor Source

The BESs fed with domestic wastewater (R_{DW}), glucose (R_{Glu}), and acetate (R_{Ac}) presented similar and commendable decolorization efficiency (>98%) with azo dye AO 7 loading rates increased from 200 to 800 g/(m³·d). The COD consumptions among the three reactors were significantly different despite influent COD concentrations being controlled at a parallel level. The highest COD removal efficiency of R_{Ac} was $39.89 \pm 1.95\%$ followed by R_{Glu} of $34.01 \pm 2.20\%$, and lowest COD removal efficiency was recorded in R_{DW} ($19.56 \pm 3.21\%$). Given the different yet similar electrons from COD oxidation used for azo dye decolorization, R_{DW} showed the highest electrons utilization efficiency. In R_{Glu} and R_{Ac} , more electrons were lost in the unwanted parallel routes, such as biomass production and methanogenesis. By decreasing electron donor concentrations from 300 to 80 mg-COD/L, the decolorization efficiencies of R_{Glu} and R_{Ac} obviously deteriorated to $85.85 \pm 2.33\%$ and $72.41 \pm 1.37\%$, respectively, which was still kept at $94.91 \pm 1.55\%$ in R_{DW} . The preferable performance of R_{DW} under lower electron donation conditions emphasized that DW could serve as a cost-efficient electron donor source to drive BES for implementing the decolorization of azo dye [14].

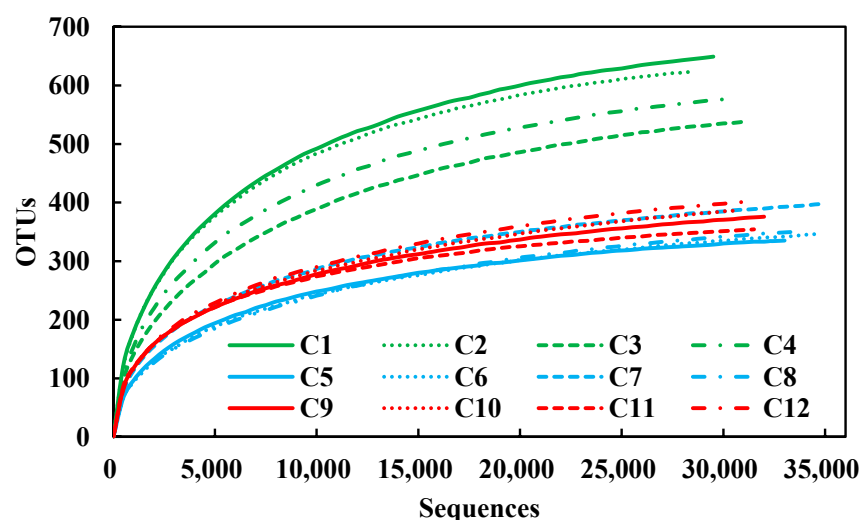
3.2. Overall Microbial Community Structures

Illumina sequencing platform was employed to analyze microbial communities from 12 electrode biofilms of three reactors, the nomenclature and alpha diversity were shown in Table 1. Approximately 30,000 high-quality sequences were obtained from each sample (Figure 2). Significantly more operational taxonomic units (OTUs) were observed in samples fed with DW, followed by glucose and acetate, respectively. It indicated that microbial diversity highly depended on the complexity of the electron donor source. The estimated species richness abundance-based coverage estimator (ACE) and Chao1 were also consistent with this trend, which was significantly higher in R_{DW} samples than that in R_{Ac} and R_{Glu} ($p < 0.05$). It implied that more species were found in R_{DW} . Shannon index was employed to evaluate the evenness of the samples and reflected that the microbial communities from R_{DW} showed better evenness. It was also confirmed by the lowest Simpson index obtained in R_{DW} samples.

Principal component analysis (PCA) demonstrated that samples from the same reactor clustered together and presented high similarity of the microbial communities (Figure 3). It is reasonable considering the process of varied electron donor source utilization. Acetate is the simplest one and can be directly utilized as an electron donor. Glucose would be fermented into volatile fatty acids and then be utilized by microbes. DW metabolic processes involve hydrolysis, acidogenesis, acetogenesis, and methanogenesis, which are operated by diverse consortia.

Table 1. Nomenclature and alpha diversity of 12 microbial communities.

Mark	Sample Name	Number of Sequences	OTU	Chao 1	ACE	Shannon	Simpson
C1	R _{DW} down-cathode	29,514	649	699	715	4.29	0.04
C2	R _{DW} down-anode	28,786	625	662	682	4.23	0.04
C3	R _{DW} up-cathode	31,281	539	592	609	3.67	0.07
C4	R _{DW} up-anode	30,224	577	629	644	3.79	0.06
C5	R _{Ac} down-cathode	33,033	335	356	373	2.80	0.17
C6	R _{Ac} down-anode	34,760	346	400	408	3.10	0.11
C7	R _{Ac} up-cathode	35,182	398	468	455	3.12	0.15
C8	R _{Ac} up-anode	33,810	351	388	415	3.30	0.08
C9	R _{Glu} down-cathode	32,182	376	421	438	3.23	0.13
C10	R _{Glu} down-anode	30,776	387	464	469	3.63	0.06
C11	R _{Glu} up-cathode	31,687	354	383	393	3.30	0.12
C12	R _{Glu} up-anode	31,257	402	463	483	3.29	0.10

**Figure 2.** Rarefaction curves of the microbial communities.

Hierarchical cluster analysis was used to identify the differences of 12 microbial communities, as shown in Figure 4. Overall, microbial communities from R_{Ac} and R_{Glu} were relatively similar and separated from the R_{DW} group, suggesting clear distinctions of community structure between the complex feeding reactor and simple one. This was consistent with PCA results. In R_{Ac} and R_{Glu}, the microbial communities from the same polarity of electrode biofilm clustered together even though they were located in a different position. It indicated that the electrode polarity was the major influence factor on the microbial community structures from electrode biofilms in R_{Ac} and R_{Glu}. It was different in R_{DW} where position rather than polarity seems to be the dominant influence factor on the microbial communities. It can be deduced that the electron donor source was a dominant factor that influenced the microbial community structure of electrode biofilms. Simple carbon source (NaAc and glucose) was more likely to be utilized by electricigens, which led to a decrease in diversity and an increase in similarity of biofilm microbial community structure. While serving a complex carbon source (DW), electron production requires a long and complicated metabolic pathway constructed by a more diversified microbial community structure.

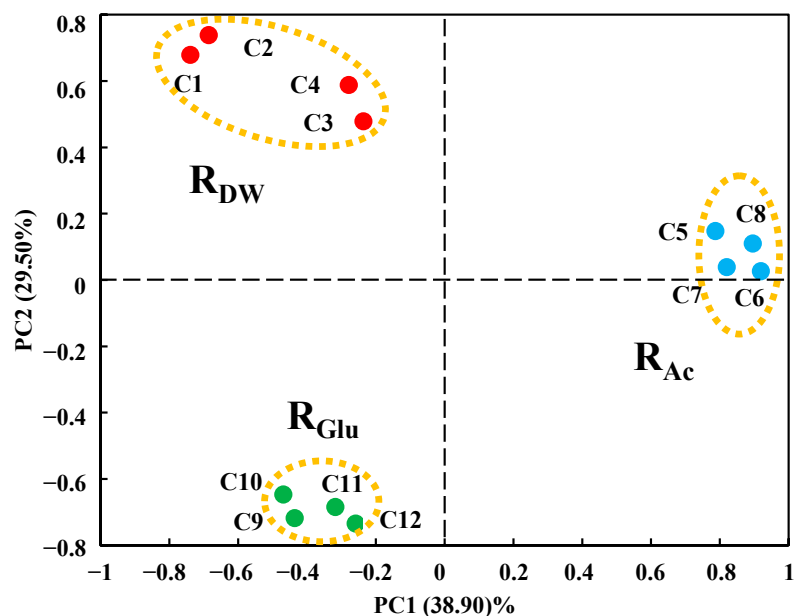


Figure 3. Principal component analysis (PCA) of microbial communities from different electron donor sources feeding BESs.

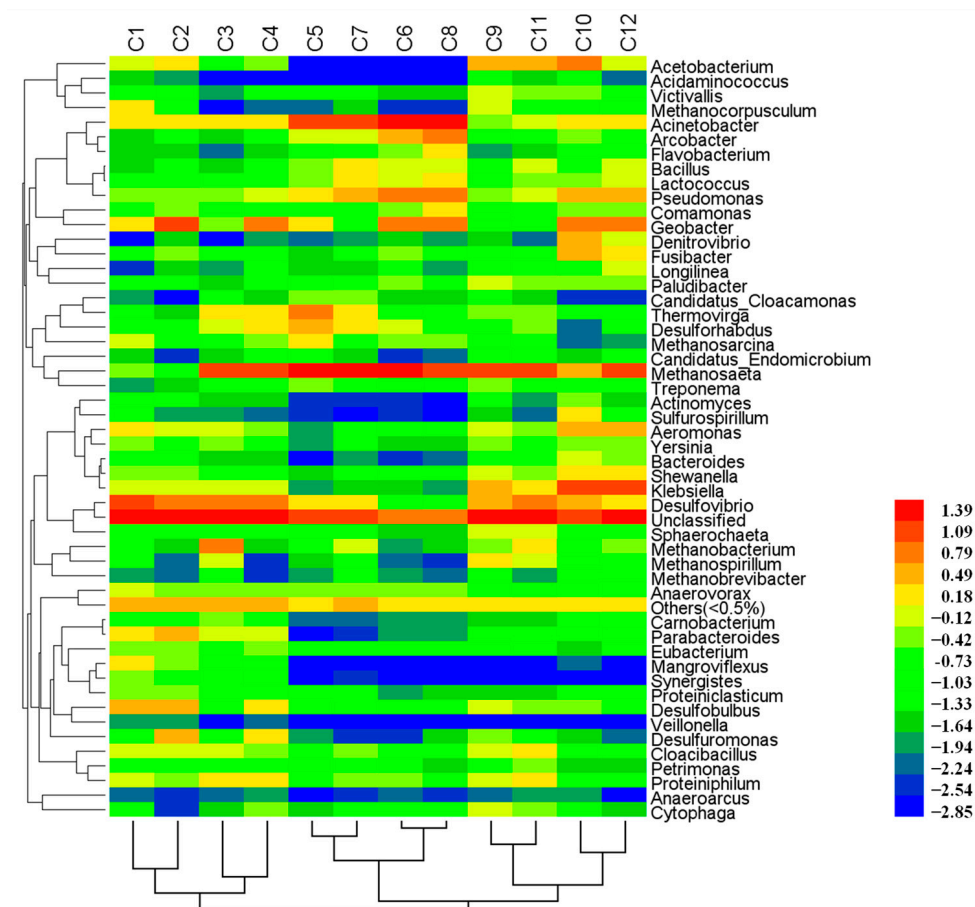


Figure 4. Hierarchical cluster analysis of microbial communities 12 biofilm samples.

3.3. Microbial Community Structures at Phylum, Class, and Family Levels

Microbial community structures from 12 samples were compared at phylum, class, and family levels (Figure 5). As it can be seen, the carbon source significantly altered the

microbial community structure. A total of 11 phyla with relative abundance >1% were identified as shown in Figure 5A. Bacteroidetes, Firmicutes, and Proteobacteria were the dominant member. Bacteroidetes was the most enriched phylum in R_{DW} with an average abundance of $31.92 \pm 3.31\%$, which was followed by $7.15 \pm 1.99\%$ and $11.52 \pm 3.22\%$ in R_{Ac} and R_{Glu} , respectively. Bacteroidetes were widely reported in BESs [17]. Firmicutes were enriched in R_{Glu} with a relative abundance of $32.65 \pm 7.18\%$. Firmicutes were frequently identified from BES that fed glucose as a carbon source [18,19]. Proteobacteria were the absolute dominant phylum in R_{Ac} ($47.22 \pm 18.13\%$), which were $29.69 \pm 11.45\%$ and $29.67 \pm 17.59\%$ in R_{DW} and R_{Glu} , respectively. In addition, Synergistota was the other relative enriched phylum with the abundances of 3.96 ± 0.98 , 2.64 ± 2.84 , and $1.31 \pm 1.12\%$ in R_{DW} , R_{Ac} , and R_{Glu} , respectively. It is worth noting that Synergistota seems to be enriched in the anode biofilm. Especially in R_{Ac} and R_{Glu} that feed with a simple carbon source, the relative abundance of Synergistota in the anode biofilm was one order of magnitude higher than the corresponding cathode. It seems to imply that the phylum of Synergistetes was relevant to the anodic respiration and extracellular electron transfer; however, there was no solid evidence to confirm this, and a deep investigation is required for illumination. A total of 18 classes were identified from 12 biofilm samples (relative abundance >1%, as shown in Figure 5B). Δ -proteobacteria with the relative abundance of $23.23 \pm 11.12\%$ was the dominant member and followed by γ -proteobacteria ($5.48 \pm 1.06\%$) in biofilms from R_{DW} , and γ -proteobacteria was the dominant class in R_{Ac} ($33.46 \pm 12.95\%$). While Bacilli, γ - and δ -proteobacteria were found to be the dominant member in biofilms in R_{Glu} with a relative abundance of $22.40 \pm 9.67\%$, $18.23 \pm 13.33\%$, and $9.89 \pm 2.93\%$, respectively.

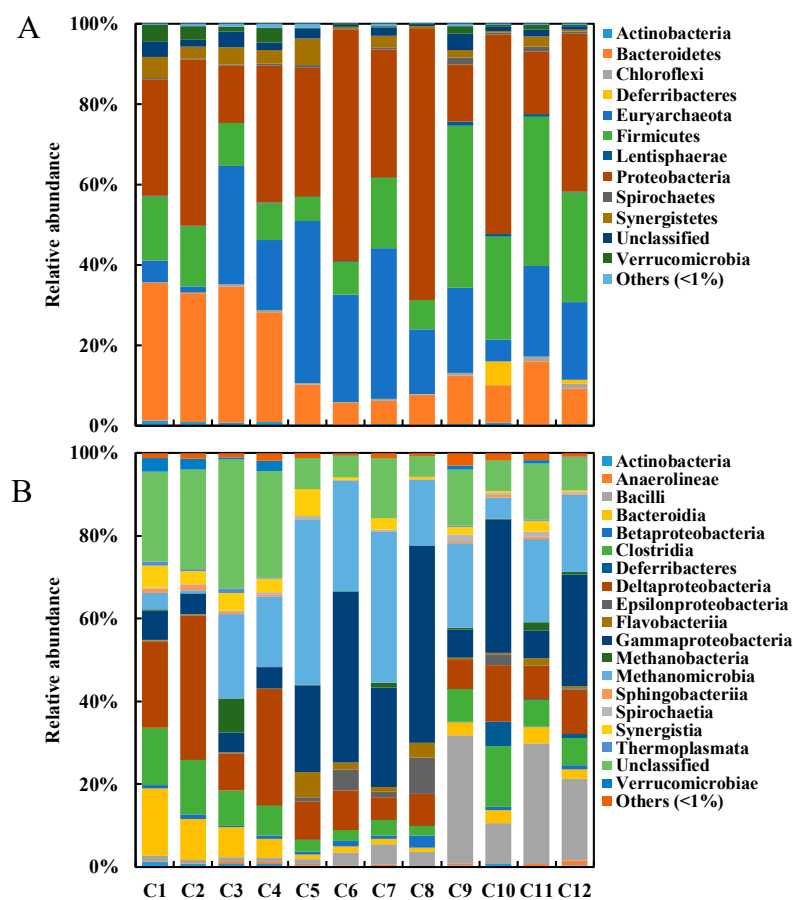


Figure 5. Microbial community comparison at phylum (A) and class (B) level.

3.4. Potential Function of Dominant Genera

An in-depth characterization of microbial community was performed at a genus level. Thirty-one genera with relative abundance >1% in the twelve microbial communities are shown in Table 2. *Geobacter*, a typical exoelectrogen, was found to be the dominant member in all anodic biofilms with the relative abundance in a range of 6.75% and 14.15%, which was higher than their corresponding cathodic biofilms. *Geobacter sulfurreducens* was the first reported strain in which microbial electricity production occurred solely by cells attached to an electrode [20]. In addition, the azo dye reduction capability of *Geobacter* has also been discovered [21].

Table 2. Microbial community comparison at genus level.

Genus	C1	C2	C3	C4	C5	C6	C7	C8	C9	C10	C11	C12
<i>Methanosaeta</i>	0.70	0.27	19.00	16.46	37.25	26.26	35.83	15.43	17.29	4.84	18.94	18.51
<i>Acinetobacter</i>	1.53	1.67	1.68	2.03	18.76	32.89	18.26	38.51	0.74	2.57	1.38	2.50
<i>Pseudomonas</i>	0.55	0.48	0.51	0.86	2.05	7.80	5.21	8.35	0.59	4.99	1.46	3.54
<i>Geobacter</i>	1.65	14.15	0.46	11.84	1.71	8.35	0.35	6.75	0.26	8.02	0.12	7.68
<i>Arcobacter</i>	0.04	0.08	0.04	0.08	1.09	5.14	1.23	8.76	0.07	0.75	0.11	0.32
<i>Thermovirga</i>	0.16	0.03	2.16	1.86	6.34	0.16	1.98	0.29	0.47	0.09	0.52	0.07
<i>Desulforhabdus</i>	0.19	0.32	1.49	1.73	4.90	0.76	2.70	0.28	0.31	0.01	0.39	0.14
<i>Desulfovibrio</i>	13.96	11.99	6.30	8.31	1.88	0.16	2.00	0.26	4.71	4.84	6.50	2.23
<i>Desulfohalobium</i>	4.34	3.82	0.15	2.16	0.29	0.07	0.18	0.07	1.00	0.55	0.51	0.36
<i>Methanobacterium</i>	0.26	0.04	8.07	0.03	0.05	0.02	1.04	0.04	0.43	0.07	1.81	0.45
<i>Parabacteroides</i>	2.19	3.51	0.88	1.32	-	0.02	0.01	0.01	0.15	0.36	0.10	0.13
<i>Desulfuromonas</i>	0.12	3.93	0.36	2.90	0.02	0.00	0.01	0.04	0.48	0.05	0.24	0.01
<i>Klebsiella</i>	1.24	0.82	1.07	0.78	0.02	0.04	0.04	0.01	3.24	17.43	2.44	15.33
<i>Acetobacterium</i>	1.30	1.65	0.17	0.51	-	-	0.00	-	4.87	7.27	3.28	1.22
<i>Aeromonas</i>	2.52	1.04	0.82	0.69	0.02	0.21	0.05	0.13	0.89	4.03	0.62	3.16
<i>Denitrovibrio</i>	-	0.02	-	0.02	0.01	0.03	0.01	0.02	0.04	5.94	0.01	1.01
<i>Fusibacter</i>	0.31	0.54	0.29	0.20	0.04	0.70	0.17	0.21	0.08	3.41	0.12	2.94
<i>Proteiniphilum</i>	1.00	0.52	2.35	1.86	0.30	0.43	0.48	0.13	1.01	0.18	2.22	0.17
<i>Cloacibacillus</i>	1.40	1.18	1.04	0.57	0.19	0.32	0.71	0.20	1.17	0.16	1.91	0.23
<i>Mangroviflexus</i>	2.58	0.39	0.10	0.06	-	-	-	-	-	0.01	-	-
<i>Anaerovorax</i>	1.22	0.56	0.73	0.51	0.52	0.38	0.60	0.48	0.23	0.19	0.14	0.12
<i>Methanocorpusculum</i>	2.02	0.29	-	0.01	0.01	0.00	0.04	0.00	1.12	0.10	0.18	0.09
<i>Methanosarcina</i>	1.05	0.20	0.17	0.63	2.76	0.49	0.29	0.56	0.06	0.01	0.10	0.02
<i>Shewanella</i>	0.53	0.50	0.32	0.22	0.03	0.14	0.09	0.13	0.80	2.38	0.62	1.50
<i>Comamonas</i>	0.31	0.43	0.13	0.31	0.32	0.56	0.26	2.08	0.08	0.49	0.11	0.65
<i>Methanospirillum</i>	0.24	0.01	0.89	0.00	0.04	0.01	0.25	0.00	1.82	0.19	0.97	0.06
<i>Lactococcus</i>	0.09	0.07	0.10	0.15	0.47	1.44	2.11	1.62	0.14	0.41	0.60	0.93
<i>Bacteroides</i>	0.10	0.15	0.03	0.03	-	0.00	0.02	0.01	0.29	1.16	0.21	0.65
<i>Bacillus</i>	0.04	0.05	0.04	0.13	0.42	1.31	2.00	1.44	0.06	0.34	0.79	1.03
<i>Sulfurospirillum</i>	0.07	0.02	0.02	0.01	0.00	0.00	-	-	0.03	1.59	0.01	0.09
<i>Flavobacterium</i>	0.04	0.03	0.01	0.03	0.12	0.69	0.33	2.89	0.02	0.08	0.03	0.06
Unclassified	49.70	44.25	43.67	36.64	15.93	8.01	18.17	7.63	49.76	21.83	47.64	28.93
Others # (<1%)	8.53	6.99	6.95	7.09	4.48	3.59	5.58	3.66	7.80	5.69	5.89	5.85

Dominant genera (>5%) in electrode biofilms were bolded; #: genus relative abundance less than 1% were classified as "Others"; "0.00": genus that identified yet low relative abundance; "-": genus that were undetected in electrode biofilms.

In the R_{DW} group, *Desulfovibrio* was enriched (13.96, 11.99, 6.30, and 8.31%) compared to R_{Ac} and R_{Glu} . *Desulfovibrio* has been proved as a functional genus for extracellular electron transfer (EET) and azo dye reduction [22,23]. It was interesting that the *Desulfovibrio* relative abundance of the microbial community was more sensitive to the electrode position rather than polarity, which was selectively enriched in the biofilms collected from down position electrodes. It is reasonable considering that this genus can grow with a broad range and as complex organic matters with electron donors [24], and it is adaptable to the complex composition of DW.

Acinetobacter is non-fermentive and capable of growth in mineral media with acetate as the sole carbon source [25]. It seems to be the reason that *Acinetobacter* was the dominant member in all samples from the R_{Ac} group. *Acinetobacter* was selectively enriched in anodic biofilm with relative abundances of 32.89 and 38.51%, which decreased to 18.76 and 18.26% in cathodic ones. It strongly implied that *Acinetobacter* was involved in electrode respiration; however, we failed to find out an explicit report to confirm the direct link between

Acinetobacter and EET. *Acinetobacter* presented function in azo dye decolorization [26]. *Pseudomonas*, a reported exoelectrogen as well as an azo dye decolorizing genus, was selected enriched in anodic biofilms (7.80% and 8.35%) versus cathodes (2.05% and 5.21%), which can produce phenazine-based metabolites to stimulate EET [27,28]. In addition, *Arcobacter* was another exoelectrogen that had high relative abundances in R_{Ac} electrodes (1.09%, 5.14%, 1.23%, and 8.76%). It has been verified that they were neither fermented nor oxidized carbohydrates, yet organic and amino acids could be utilized as carbon sources [29,30].

In the R_{Glucose} group, *Klebsiella* was the dominant member with relative abundances of 17.43% and 15.33% in anodes and one order of magnitude lower (3.24% and 2.44%) in cathodes. It is a functional genus of EET and azo dye reduction [31,32]. *Acetobacterium* was an enriched genus in R_{Glucose} group, with relative abundances of 4.87%, 7.27%, 3.28%, and 1.22%. *Acetobacterium* was not proved for its function in EET or azo dye reduction; however, it was an acetogenic microbe and can produce acetate by oxidizing glucose [33].

In terms of archaea, *Methanosaeta* was the predominant methane producer that specializes in only using acetate for methane production. No growth on or methane production from H₂/CO₂, formate, methanol, ethanol, trimethylamine, isobutanol, or isopropanol [34] was observed. This explains the enrichment of *Methanosaeta* on the R_{Ac} biofilms (37.25%, 26.26%, 35.83%, and 15.43%). The relative abundances of *Methanosaeta* were lower in the R_{DW} and R_{Glucose} groups and relatively enriched in the down electrode biofilms. Both DW and glucose should be fermented in acetate to create a favorable condition for *Methanosaeta* metabolism so that they are relatively enriched on the up electrodes. The recent literature indicated *Methanosaeta* is able to acquire electrons from exoelectrogen (e.g., *Geobacter*) by direct interspecies electron transfer process [35,36]. In addition, *Methanosaeta* was found to be a dominant member in a microbial community from an anaerobic baffled reactor treating dyes wastewater, which implied it could tolerate the toxicity of the dyes and possibly be involved in dye removal. Other methane producers, *Methanobacterium*, *Methanocorpusculum*, *Methanosarcina*, and *Methanospirillum*, were found but with quite lower relative abundances in 12 biofilms.

Canonical correspondence analysis (CCA) was employed to evaluate the effect of electron donor source types on the microbial community structures, as shown in Figure 6. The arrow direction of acetate was positively correlated with the horizontal canonical axis, and DW and glucose were located in the middle of the second and third quadrant of the cartesian coordinate. The separation of three electron donor sources indicated the relatively independent selective pressure. *Mangroviflexus* stood in the DW direction and far away from the origin, and its enrichment was highly sensitive to DW. It was a dominant genus in the rural household biogas digesters and played a crucial role in reducing and oxidizing reactions to bio-degrade organic matters [37]. *Parabacteroides* was an obligately anaerobic species from wastewater of a paper mill [38]. *Desulfuromonas* was able to oxidize complex organics such as long-chain fatty acids and use tetrachloroethylene, trichloroethylene, and Fe(III) as electron acceptors [39,40]. *Klebsiella* had a function of EET from glucose oxidation [41]; thus, it was enriched on the anodes from R_{Glucose}. *Acinetobacter*, *Arcobacter*, and *Flavobacterium* were highly sensitive to the acetate.

The comparisons of the dominant genera that were identified from BESs fed with various electron donor sources are summarized in Table S1 [42–45]. It is quite clear that the genera with a function of extracellular electron transfer, such as *Geobacter*, *Pseudomonas*, *Desulfovibrio*, and *Klebsiella*, were enriched in the electrode microbial community. Those genera seemed to endow an electrochemical activity of the electrode biofilms. Specific genus was enriched based on the characteristics of the substrate. *Comamonadaceae* was enriched in a BES with phenol as the substrate [45], and *Klebsiella* was enriched in this work with domestic wastewater as the electron donor.

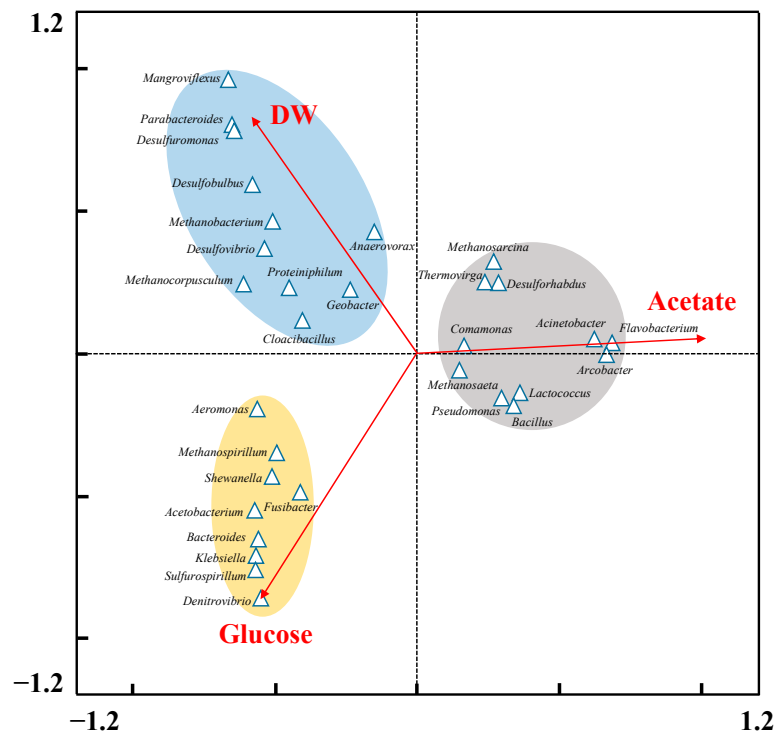


Figure 6. Canonical correspondence analysis for electron donor sources and functional genera from electrode microbial communities.

4. Conclusions

Employing domestic wastewater as electron donor source to drive bioelectrochemical reaction was feasible and cost-efficient. In this study, the electrode microbial communities from bioelectrochemical systems fed with domestic wastewater (R_{DW}), acetate (R_{Ac}), and glucose (R_{Glu}) were systematically revealed. Similar decolorization performances were observed among three BESs, while the microbial community structures were quite different. Microbial diversity highly depended on the complexity of the electron donor source, and significantly more OTUs were observed in R_{DW} compared to R_{Glu} and R_{Ac} . Bacteroidetes, Firmicutes, and Proteobacteria were identified as the dominated phyla in R_{DW} , R_{Glu} , and R_{Ac} , respectively. *Desulfovibrio*, *Acinetobacter*, and *Klebsiella* were identified as the predominant bacterial genera in R_{DW} , R_{Ac} , and R_{Glu} , respectively. Typical exoelectrogen *Geobacter* was found to be enriched in the anodes' biofilms among three BES reactors. *Methanosaeta* was the most enriched methanogen in all reactors. This study provides an insight in the microbial response mechanism to the electron donor sources and provides great inspiration to bring bioelectrochemical technology closer to applications.

Supplementary Materials: The following supporting information can be downloaded at: <https://www.mdpi.com/article/10.3390/w14091505/s1>, Table S1: Comparison of dominant genera fed with various electron donor sources.

Author Contributions: Z.G.: Investigation, funding acquisition, and writing—review and editing. L.Z.: Investigation and writing—original draft. M.-H.C.: Conceptualization, funding acquisition, and writing—review and editing. A.W.: Project administration and supervision. All authors have read and agreed to the published version of the manuscript.

Funding: This research was funded by the Natural Science Foundation of Jiangsu Province, No. BK20190980; the National Natural Science Foundation of China, No. 52000090 and 52000088; the China Postdoctoral Science Foundation, No. 2021M701511; the Open Project of Key Laboratory of Environmental Biotechnology, CAS, Grant No. kf2020010.

Institutional Review Board Statement: Not applicable.

Informed Consent Statement: Not applicable.

Data Availability Statement: Not applicable.

Conflicts of Interest: The authors declare no conflict of interest.

References

1. Suprun, E.V.; Radko, S.P.; Khmeleva, S.A.; Mitkevich, V.A.; Archakov, A.I.; Makarov, A.A.; Shumyantseva, V.V. Electrochemical oxidation of amyloid-beta peptide isoforms on carbon screen printed electrodes. *Electrochem. Commun.* **2017**, *75*, 33–37. [[CrossRef](#)]
2. Kong, D.; Liang, B.; Yun, H.; Cheng, H.; Ma, J.; Cui, M.; Wang, A.; Ren, N. Cathodic degradation of antibiotics: Characterization and pathway analysis. *Water Res.* **2015**, *72*, 281–292. [[CrossRef](#)] [[PubMed](#)]
3. Cui, M.-H.; Liu, W.-Z.; Tang, Z.-E.; Cui, D. Recent advancements in azo dye decolorization in bio-electrochemical systems (BESs): Insights into decolorization mechanism and practical application. *Water Res.* **2021**, *203*, 117512. [[CrossRef](#)]
4. Cui, M.-H.; Cui, D.; Gao, L.; Cheng, H.-Y.; Wang, A.-J. Analysis of electrode microbial communities in an up-flow bioelectrochemical system treating azo dye wastewater. *Electrochim. Acta* **2016**, *220*, 252–257. [[CrossRef](#)]
5. Tang, C.-C.; Zhang, X.-Y.; Wang, R.; Wang, T.-Y.; He, Z.-W.; Wang, X.C. Calcium ions-effect on performance, growth and extracellular nature of microalgal-bacterial symbiosis system treating wastewater. *Environ. Res.* **2022**, *207*, 112228. [[CrossRef](#)] [[PubMed](#)]
6. Zieliński, M.; Dębowski, M.; Kazimierowicz, J. Microwave Radiation Influence on Dairy Waste Anaerobic Digestion in a Multi-Section Hybrid Anaerobic Reactor (M-SHAR). *Processes* **2021**, *9*, 1772. [[CrossRef](#)]
7. Westerholm, M.; Crauwels, S.; Van Geel, M.; Dewil, R.; Lievens, B.; Appels, L. Microwave and ultrasound pre-treatments influence microbial community structure and digester performance in anaerobic digestion of waste activated sludge. *Appl. Microbiol. Biotechnol.* **2016**, *100*, 5339–5352. [[CrossRef](#)]
8. Dębowski, M.; Zieliński, M.; Kisielewska, M.; Kazimierowicz, J. Evaluation of Anaerobic Digestion of Dairy Wastewater in an Innovative Multi-Section Horizontal Flow Reactor. *Energies* **2020**, *13*, 2392. [[CrossRef](#)]
9. Lyu, W.; Song, Q.; Shi, J.; Wang, H.; Wang, B.; Hu, X. Weak magnetic field affected microbial communities and function in the A/O/A sequencing batch reactors for enhanced aerobic granulation. *Sep. Purif. Technol.* **2021**, *266*, 118537. [[CrossRef](#)]
10. Zhao, B.; Sha, H.; Li, J.; Cao, S.; Wang, G.; Yang, Y. Static magnetic field enhanced methane production via stimulating the growth and composition of microbial community. *J. Clean. Prod.* **2020**, *271*, 122664. [[CrossRef](#)]
11. Daghighi, M.; Gandolfi, I.; Bestetti, G.; Franzetti, A.; Guerrini, E.; Cristiani, P. Anodic and cathodic microbial communities in single chamber microbial fuel cells. *New Biotechnol.* **2015**, *32*, 79–84. [[CrossRef](#)] [[PubMed](#)]
12. Zhai, S.; Ji, M.; Zhao, Y.; Pavlostathis, S.G.; Zhao, Q. Effects of salinity and COD/N on denitrification and bacterial community in dicyclic-type electrode based biofilm reactor. *Chemosphere* **2017**, *192*, 328–336. [[CrossRef](#)] [[PubMed](#)]
13. Zhu, X.; Yates, M.D.; Hatzell, M.C.; Rao, H.A.; Saikaly, P.E.; Logan, B.E. Microbial Community Composition Is Unaffected by Anode Potential. *Environ. Sci. Technol.* **2013**, *48*, 1352–1358. [[CrossRef](#)] [[PubMed](#)]
14. Cui, M.-H.; Cui, D.; Gao, L.; Wang, A.-J.; Cheng, H.-Y. Azo dye decolorization in an up-flow bioelectrochemical reactor with domestic wastewater as a cost-effective yet highly efficient electron donor source. *Water Res.* **2016**, *105*, 520–526. [[CrossRef](#)]
15. Mu, Y.; Rabaey, K.; Rozendal, R.A.; Yuan, Z.; Keller, J. Decolorization of Azo Dyes in Bioelectrochemical Systems. *Environ. Sci. Technol.* **2009**, *43*, 5137–5143. [[CrossRef](#)]
16. Cheng, H.-Y.; Liang, B.; Mu, Y.; Cui, M.-H.; Li, K.; Wu, W.; Wang, A.-J. Stimulation of oxygen to bioanode for energy recovery from recalcitrant organic matter aniline in microbial fuel cells (MFCs). *Water Res.* **2015**, *81*, 72–83. [[CrossRef](#)]
17. Quan, X.-C.; Quan, Y.-P.; Tao, K. Effect of anode aeration on the performance and microbial community of an air-cathode microbial fuel cell. *Chem. Eng. J.* **2012**, *210*, 150–156. [[CrossRef](#)]
18. Liang, B.; Cheng, H.; Van Nostrand, J.; Ma, J.; Yu, H.; Kong, D.; Liu, W.; Ren, N.; Wu, L.; Wang, A.; et al. Microbial community structure and function of Nitrobenzene reduction biocathode in response to carbon source switchover. *Water Res.* **2014**, *54*, 137–148. [[CrossRef](#)]
19. Cui, M.-H.; Cui, D.; Lee, H.-S.; Liang, B.; Wang, A.-J.; Cheng, H.-Y. Effect of electrode position on azo dye removal in an up-flow hybrid anaerobic digestion reactor with built-in bioelectrochemical system. *Sci. Rep.* **2016**, *6*, 25223. [[CrossRef](#)]
20. Bond, D.R.; Lovley, D.R. Electricity Production by *Geobacter sulfurreducens* Attached to Electrodes. *Appl. Environ. Microbiol.* **2003**, *69*, 1548–1555. [[CrossRef](#)]
21. Liu, G.; Zhou, J.; Chen, C.; Wang, J.; Jin, R.; Lv, H. Decolorization of azo dyes by *Geobacter metallireducens*. *Appl. Microbiol. Biotechnol.* **2012**, *97*, 7935–7942. [[CrossRef](#)] [[PubMed](#)]
22. Kang, C.S.; Eaktasang, N.; Kwon, D.-Y.; Kim, H.S. Enhanced current production by *Desulfovibrio desulfuricans* biofilm in a mediator-less microbial fuel cell. *Bioresour. Technol.* **2014**, *165*, 27–30. [[CrossRef](#)]
23. Kim, S.-Y.; An, J.-Y.; Kim, B.-W. Improvement of the decolorization of azo dye by anaerobic sludge bioaugmented with *Desulfovibrio desulfuricans*. *Biotechnol. Bioprocess Eng.* **2007**, *12*, 222–227. [[CrossRef](#)]
24. Sass, H.; Ramamoorthy, S.; Yarwood, C.; Langner, H.; Schumann, P.; Kroppenstedt, R.M.; Spring, S.; Rosenzweig, R.F. *Desulfovibrio idahonensis* sp. nov., sulfate-reducing bacteria isolated from a metal(loid)-contaminated freshwater sediment. *Int. J. Syst. Evol. Microbiol.* **2009**, *59*, 2208–2214. [[CrossRef](#)] [[PubMed](#)]

25. Li, W.; Zhang, D.; Huang, X.; Qin, W. *Acinetobacter harbinensis* sp. nov., isolated from river water. *Int. J. Syst. Evol. Microbiol.* **2014**, *64 Pt 5*, 1507–1513. [[CrossRef](#)] [[PubMed](#)]
26. Cai, Z.; Zhang, W.; Ma, J.; Cai, J.; Li, S.; Zhu, X.; Yang, G.; Zhao, X. Biodegradation of Azo Dye Disperse Orange S-RL by a Newly Isolated Strain *Acinetobacter* sp. SRL8. *Water Environ. Res.* **2015**, *87*, 516–523. [[CrossRef](#)]
27. Pham, T.H.; Boon, N.; De Maeyer, K.; Höfte, M.; Rabaey, K.; Verstraete, W. Use of *Pseudomonas* species producing phenazine-based metabolites in the anodes of microbial fuel cells to improve electricity generation. *Appl. Microbiol. Biotechnol.* **2008**, *80*, 985–993. [[CrossRef](#)]
28. Qiao, Y.; Qiao, Y.-J.; Zou, L.; Ma, C.-X.; Liu, J. Real-time monitoring of phenazines excretion in *Pseudomonas aeruginosa* microbial fuel cell anode using cavity microelectrodes. *Bioresour. Technol.* **2015**, *198*, 1–6. [[CrossRef](#)]
29. Vandamme, P.; Falsen, E.; Rossau, R.; Hoste, B.; Segers, P.; Tytgat, R.; De Ley, J. Revision of *Campylobacter*, *Helicobacter*, and *Wolinella* Taxonomy: Emendation of Generic Descriptions and Proposal of *Arcobacter* gen. nov. *Int. J. Syst. Bacteriol.* **1991**, *41*, 88–103. [[CrossRef](#)]
30. Toh, H.; Sharma, V.K.; Oshima, K.; Kondo, S.; Hattori, M.; Ward, F.B.; Free, A.; Taylor, T.D. Complete Genome Sequences of *Arcobacter butzleri* ED-1 and *Arcobacter* sp. Strain L, Both Isolated from a Microbial Fuel Cell. *J. Bacteriol.* **2011**, *193*, 6411–6412. [[CrossRef](#)]
31. Lee, Y.-Y.; Kim, T.G.; Cho, K.-S. Enhancement of electricity production in a mediatorless air–cathode microbial fuel cell using *Klebsiella* sp. IR21. *Bioprocess Biosyst. Eng.* **2016**, *39*, 1005–1014. [[CrossRef](#)] [[PubMed](#)]
32. Elizalde-González, M.; Fuentes, L.; Guevara-Villa, M. Degradation of immobilized azo dyes by *Klebsiella* sp. UAP-b5 isolated from maize bioadsorbent. *J. Hazard. Mater.* **2009**, *161*, 769–774. [[CrossRef](#)] [[PubMed](#)]
33. Balch, W.E.; Schoberth, S.; Tanner, R.S.; Wolfe, R.S. *Acetobacterium*, a New Genus of Hydrogen-Oxidizing, Carbon Dioxide-Reducing, Anaerobic Bacteria. *Int. J. Syst. Bacteriol.* **1977**, *27*, 355–361. [[CrossRef](#)]
34. Ma, K. *Methanosaeta harundinacea* sp. nov., a novel acetate-scavenging methanogen isolated from a UASB reactor. *Int. J. Syst. Evol. Microbiol.* **2006**, *56 Pt 1*, 127–131. [[CrossRef](#)]
35. Liu, F.; Rotaru, A.-E.; Shrestha, P.M.; Malvankar, N.S.; Nevin, K.P.; Lovley, D.R. Promoting direct interspecies electron transfer with activated carbon. *Energy Environ. Sci.* **2012**, *5*, 8982–8989. [[CrossRef](#)]
36. Rotaru, A.-E.; Shrestha, P.M.; Liu, F.; Shrestha, M.; Shrestha, D.; Embree, M.; Zengler, K.; Wardman, C.; Nevin, K.P.; Lovley, D.R. A new model for electron flow during anaerobic digestion: Direct interspecies electron transfer to *Methanosaeta* for the reduction of carbon dioxide to methane. *Energy Environ. Sci.* **2013**, *7*, 408–415. [[CrossRef](#)]
37. Han, R.; Yuan, Y.; Cao, Q.; Li, Q.; Chen, L.; Zhu, D.; Liu, D. PCR–DGGE Analysis on Microbial Community Structure of Rural Household Biogas Digesters in Qinghai Plateau. *Curr. Microbiol.* **2017**, *75*, 541–549. [[CrossRef](#)]
38. Tan, H.-Q.; Li, T.-T.; Zhu, C.; Zhang, X.-Q.; Wu, M.; Zhu, X.-F. *Parabacteroides chartae* sp. nov., an obligately anaerobic species from wastewater of a paper mill. *Int. J. Syst. Evol. Microbiol.* **2012**, *62 Pt 11*, 2613–2617. [[CrossRef](#)]
39. Coates, J.D.; Lonergan, D.J.; Philips, E.J.P.; Jenter, H.; Lovley, D.R. *Desulfuromonas palmitatis* sp. nov., a marine dissimilatory Fe(III) reducer that can oxidize long-chain fatty acids. *Arch. Microbiol.* **1995**, *164*, 406–413. [[CrossRef](#)]
40. Krumholz, L.R. *Desulfuromonas chloroethenica* sp. nov. Uses Tetrachloroethylene and Trichloroethylene as Electron Acceptors. *Int. J. Syst. Bacteriol.* **1997**, *47*, 1262–1263. [[CrossRef](#)]
41. Xia, X.; Cao, X.-X.; Liang, P.; Huang, X.; Yang, S.-P.; Zhao, G.-G. Electricity generation from glucose by a *Klebsiella* sp. in microbial fuel cells. *Appl. Microbiol. Biotechnol.* **2010**, *87*, 383–390. [[CrossRef](#)] [[PubMed](#)]
42. Yu, Y.-Y.; Zhen, S.-H.; Chao, S.-L.; Wu, J.; Cheng, L.; Li, S.-W.; Xiao, X.; Zhou, X. Electrochemistry of newly isolated Gram-positive bacteria *Paenibacillus lautus* with starch as sole carbon source. *Electrochim. Acta* **2022**, *411*, 140068. [[CrossRef](#)]
43. Mai, Q.; Yang, G.; Cao, J.; Zhang, X.; Zhuang, L. Stratified microbial structure and activity within anode biofilm during electrochemically assisted brewery wastewater treatment. *Biotechnol. Bioeng.* **2020**, *117*, 2023–2031. [[CrossRef](#)] [[PubMed](#)]
44. Wang, Y.; Pan, Y.; Zhu, T.; Wang, A.; Lu, Y.; Lv, L.; Zhang, K.; Li, Z. Enhanced performance and microbial community analysis of bioelectrochemical system integrated with bio-contact oxidation reactor for treatment of wastewater containing azo dye. *Sci. Total Environ.* **2018**, *634*, 616–627. [[CrossRef](#)] [[PubMed](#)]
45. Yang, L.-H.; Cheng, H.-Y.; Ding, Y.-C.; Su, S.-G.; Wang, B.; Zeng, R.; Sharif, H.M.A.; Wang, A.-J. Enhanced treatment of coal gasification wastewater in a membraneless sleeve-type bioelectrochemical system. *Bioelectrochemistry* **2019**, *129*, 154–161. [[CrossRef](#)]